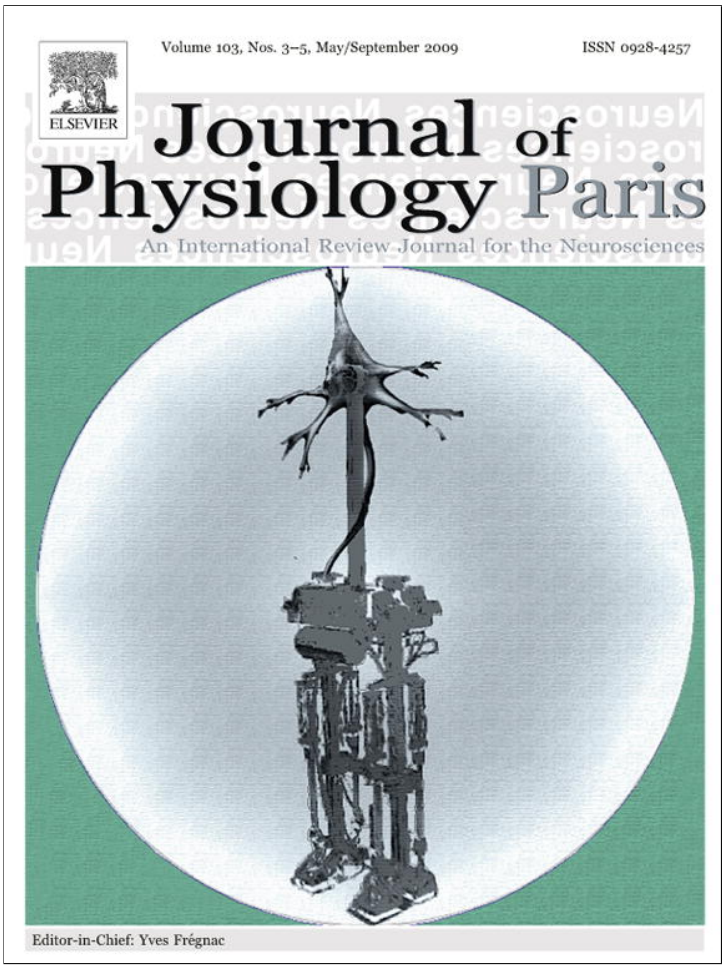

Journal of Physiology - Paris 103 (2009) 244–254

Contents lists available at ScienceDirect

Journal of Physiology - Paris

journal homepage: www.elsevier.com/locate/jphysparis

A review on directional information in neural signals for brain-machine interfaces

Stephan Waldert [a,b,*,1], Tobias Pistohl [a,b,1], Christoph Braun [c,d], Tonio Ball [a,b,e], Ad Aertsen [a,b], Carsten Mehring [a,b,*]

[a] Faculty of Biology, Albert-Ludwigs-University, Hauptstr. 1, 79104 Freiburg, Germany
[b] Bernstein Center for Computational Neuroscience, Hansastr. 9a, 79104 Freiburg, Germany
[c] MEG-Center, University of Tübingen, Tübingen, Germany
[d] CIMeC, Center of Mind/Brain Sciences, University of Trento, Trento, Italy
[e] Epilepsy Center, University Clinics, Albert-Ludwigs University, Freiburg, Germany

ARTICLE INFO

Keywords:
Directional tuning
Decoding
SUA
MUA
LFP
ECoG
EEG
MEG
BMI
BCI

ABSTRACT

Brain-machine interfaces (BMIs) can be characterized by the technique used to measure brain activity and by the way different brain signals are translated into commands that control an effector. We give an overview of different approaches and focus on a particular BMI approach: the movement of an artificial effector (e.g. arm prosthesis to the right) by those motor cortical signals that control the equivalent movement of a corresponding body part (e.g. arm movement to the right). This approach has been successfully applied in monkeys and humans by accurately extracting parameters of movements from the spiking activity of multiple single-units. Here, we review recent findings showing that analog neuronal population signals, ranging from intracortical local field potentials over epicortical ECoG to non-invasive EEG and MEG, can also be used to decode movement direction and continuous movement trajectories. Therefore, these signals might provide additional or alternative control for this BMI approach, with possible advantages due to reduced invasiveness.

1. Introduction

1.1. Brain-machine interfaces

A brain-machine interface (BMI), also referred to as brain-computer interface (BCI), is a device that translates neural activity of the brain into commands driving a machine (see Fig. 1). Three major parts constitute a BMI:

(1) A device to record neural activity from the brain. The recording can be invasive or non-invasive and different kinds of signals (e.g. spiking activity of single or multiple neurons, analog neural population signals like field potentials) can be measured. The nature of these recordings can impose certain constraints on the implementation and potential capabilities of a BMI, some of which will be discussed in this article.
(2) An effector which is controlled by the neural signals. The effector can be anything from a visual signal (e.g. computer cursor) to a complicated robotic or prosthetic system.
(3) An algorithm that analyzes and interprets the neural signals as control commands. This algorithm links the other two parts together. It determines which features of the recorded neural activity will be employed – and therefore should be produced by the user – and which control commands can be created from the activity. As such it is of great importance in defining the possible functions of the actual interface.

Applications of BMIs are mainly seen in, although not limited to, the field of rehabilitation and medical care for paralyzed patients; either with the intent to establish a novel communication channel for severely paralyzed patients in order to restore social interaction or as a means to drive prosthetic devices to restore movement capabilities. If forthcoming prostheses will allow for more degrees of freedom than those currently available, major challenges are the generation of appropriate high-dimensional neural control commands by the user and their correct interpretation by an automated interface. The quality of BMI mediated control obtained in

* Corresponding authors. Address: Faculty of Biology, Hauptstr. 1, 79104 Freiburg, Germany. Tel.: +49 761 203 2542; fax: +49 761 203 2921 (S. Walbert), tel.: +49 761 203 2543; fax: +49 761 203 2921 (C. Mehring).
E-mail addresses: waldert@bccn.uni-freiburg.de (S. Waldert), tobias.pistohl@biologie.uni-freiburg.de (T. Pistohl), christoph.braun@uni-tuebingen.de (C. Braun), tonio.ball@uniklinik-freiburg.de (T. Ball), aertsen@biologie.uni-freiburg.de (A. Aertsen), mehring@biologie.uni-freiburg.de (C. Mehring).
[1] These authors contributed equally to the manuscript.

0928-4257/$ - see front matter © 2009 Elsevier Ltd. All rights reserved.
doi:10.1016/j.jphysparis.2009.08.007

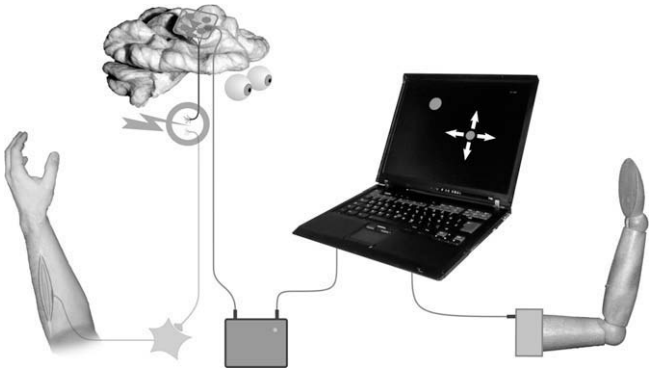

Fig. 1. General scheme of a brain-machine interface (BMI) for restoration of motor control: while in healthy people the output of neural activity in the motor cortex is conveyed to motor neurons in the spinal cord and from there to the muscles, ultimately controlling a limb, this connection might be interrupted due to injuries or neuro-degenerative diseases. A BMI reads the activity of neuronal ensembles and transmits it to a computer program, which then interprets this activity as commands to control an effector (e.g. an artificial limb).

this way should be as close as possible to the natural control of a limb.

1.2. Different BMI approaches

A major question in BMI research is: which brain signal should be used and translated into control commands driving external effectors? Different approaches have been developed and applied in the past. In what follows we will differentiate prominent methods by the recording technique used and by the specific mental task or strategy involved.

1.2.1. Recording techniques

Current techniques involve recordings of action potentials of single neurons up to recordings of superimposed neural activity of large groups of neurons (see Fig. 2). The most spatially resolved information can be obtained by implanting microelectrode arrays into the cortex. Such extracellular recordings capture spike signals and local field potentials from neurons in the close vicinity of each electrode tip. From these signals, the following three BMI input signals can be derived: single-unit activity (SUA), multi-unit activity (MUA), and local field potentials (LFP). SUA is obtained by high-pass filtering (>ca. 300 Hz) of the extracellular potential, spike detection and spike sorting i.e., assigning each spike to its corresponding neuron. MUA is obtained in the same way but without spike sorting i.e., the signal can consist of spikes originating from multiple neurons. The spiking activity measured with SUA and MUA can be reduced to discrete events in time. LFPs are extracted by low-pass filtering (<ca. 300 Hz) of the extracellular potential and are assumed to reflect mainly synaptic input to the neuronal population in the vicinity of the electrode tip. LFPs are analog signals. An alternative to recording SUA and MUA using conventional microelectrodes is to use intracortical neurotrophic electrodes (Kennedy and Bakay, 1998), where axonal outgrowth is guided by growth factors inside a glass cone. The spikes transmitted in those axons are then recorded via an electrode inside the glass cone.

On the next level, regular grids or stripes of electrodes are implanted subdurally on the surface of the cortex, or also epidurally. The electrocorticogram (ECoG) recorded with this invasive technique reflects synaptic inputs to the neuronal population beneath each electrode. The ECoG, like the LFP and the following signal types, is an analog signal.

Similar signals, but at a lower spatial resolution can be recorded non-invasively using electroencephalography (EEG) on the scalp or magnetoencephalography (MEG). Both signals reflect the activity of large neuronal populations. In contrast to EEG, which reflects extracellular currents, MEG reflects intracellular currents flowing through dendrites which produce magnetic fields measurable outside the head.

Alternatively, the non-invasive recording techniques functional magnetic resonance imaging (fMRI) and functional near-infrared spectroscopy (fNIRS) measure neural activity indirectly i.e., based on the blood oxygenation level. These two techniques have also been used for BMIs but due to the nature of these signals they exhibit a substantially lower temporal resolution.

1.2.2. Mental task or strategy

Several different mental tasks and strategies have been applied in non-invasive BMIs, mainly using EEG as a recording technique.

A wide-spread approach uses movement imagination of different parts of the body (Pfurtscheller et al., 1993; Pfurtscheller and Neuper, 2006; Blankertz et al., 2007). Due to the somatotopic organization of the primary motor cortex, such imagined movements cause characteristic spatial activation patterns that are distinguish-

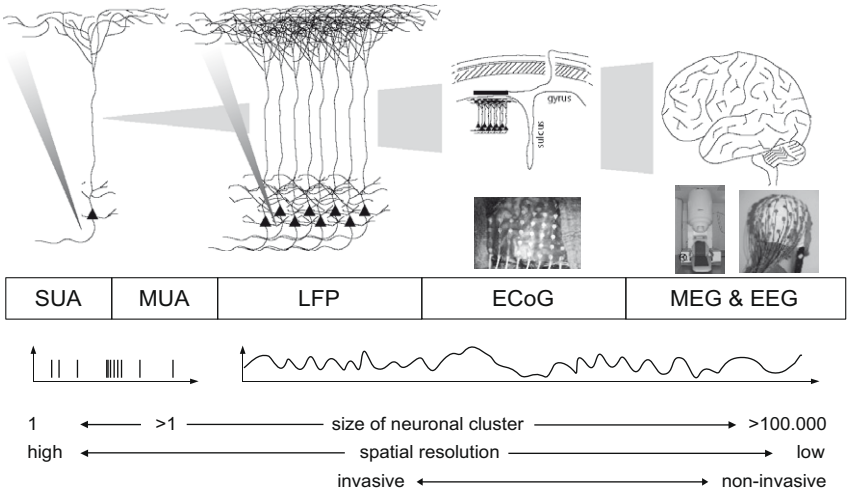

Fig. 2. Schematic overview of the recording techniques SUA/MUA, LFP, ECoG, and MEG/EEG showing (from top to bottom): the spatial scale at which signals are recorded, the characteristic of the signal (discrete vs. analog), and the correspondence to different scales.

able by classification algorithms and, therefore, can be used to control an external effector.

Another group of approaches uses self-regulation of brain-activity which can be learned by neurofeedback training. Here, for instance, the voluntary up- and down-regulation of slow-cortical potentials (Birbaumer et al., 1999) via an arbitrary subject-dependent strategy provides appropriate control signals. In a similar way, voluntary modulation of the amplitude of different frequency bands (mainly mu – ~8–12 Hz or beta – ~15–30 Hz (Wolpaw et al., 1991; Wolpaw and McFarland, 2004; McFarland et al., 2008)), often mediated by movement imagination, has been used.

Besides these approaches, also the mental execution of different cognitive tasks (Penny and Roberts, 1999; Curran et al., 2004), such as adding numbers against music imagination, provide distinguishable brain signals for BMI control.

Similar approaches (movement imagination and cognitive tasks) are also used in fMRI/fNIRS BMIs (Yoo et al., 2004; Sitaram et al., 2007).

Distinct from the aforementioned self-paced approaches are those using brain activity elicited as a response to external stimuli: among these externally-paced BMIs are those based on the steady-state visual evoked potential (SSVEP; Middendorf et al., 2000; Allison et al., 2008) and the P300. The SSVEP refers to a periodic signal elicited in the occipital cortex when the subject is focusing on a flickering visual stimulus (6–8 Hz or more). The oscillation frequency of the SSVEP is driven by that of the attended stimulus, which allows the subject to select one out of several simultaneously presented stimuli flickering with different frequencies. The P300 refers to a (positive) EEG deflection around 300 ms after presentation of a rare stimulus the subject is attending to. If a set of distinct visual (Farwell and Donchin, 1988; Hoffmann et al., 2008) or auditory (Sellers et al., 2006) stimuli are presented sequentially, the P300 indicates the stimulus selected by the subjects and, thus, also enables a BMI to convey the subject's request.

1.2.3. Direct motor BMI

In the field of invasive BMIs using spiking activity, primarily a different approach is applied: the neural activation pattern of several single neurons, related to movements of one limb, is used to achieve an equivalent control of an external effector (Serruya et al., 2002; Taylor et al., 2002; Carmena et al., 2003; Velliste et al., 2008). Throughout this review, we will use the term 'direct motor BMI' to address this kind of approach, independent of the neural signal used. Such direct motor BMI control turned out to be precise (see citations above). It is also intuitive, as neural commands for limb and external effector movements mainly match and, therefore, an arbitrary association between brain activity and the effector's behavior does not have to be learned. Thus, it can require less intensive subject training than approaches based on learned self-regulation of brain activity. The direct motor BMI approach is based on findings in monkey studies (Georgopoulos et al., 1983, 1986; Moran and Schwartz, 1999), which showed that the direction and also the speed of performed arm movements can be inferred from firing rates of motor cortical neurons. Similarly, for the human motor cortex it has been shown that the firing rates of neurons are tuned to the direction of intended hand movements (Hochberg et al., 2006). Recently, BMI research revealed that movement directions can not only be inferred from SUA but also from monkey MUA and LFP (Mehring et al., 2003), human ECoG (Leuthardt et al., 2004; Mehring et al., 2004), and human EEG and MEG (Waldert et al., 2008) i.e., the directional tuning of neural activity in motor areas was demonstrated to exist from single cell spiking activity, measured intracortically, up to superimposed activity of large groups of neurons measured non-invasively. In the following, we will discuss this directional tuning of different neuronal signals in detail.

2. Directional tuning

A variety of neural signals consistently vary with the direction of arm movements. In humans and other primates this has often been assessed with the help of so-called center-out movement experiments (see Fig. 3A), where the subject performs hand-arm movements from a central origin to one of several target positions arranged around the origin.

2.1. Directional tuning in spiking signals: SUA and MUA

In 1982, Georgopoulos et al. found for individual neurons in the primary motor cortex a systematic dependency of the firing rate on the direction of arm movements when monkeys performed two-dimensional center-out movements to eight different targets (Georgopoulos et al., 1982), as shown in Fig. 4A. The dependency of firing rates on movement direction could be approximated by a cosine function (cosine tuning). For each directionally tuned neuron, the movement direction that evokes the highest firing-rate is the so-called preferred direction of that neuron. Using the firing rates of many neurons – each one giving a 'vote' according to its preferred direction and firing rate – it is possible to compute the so-called population vector that points in the direction of the performed movement (Georgopoulos et al., 1983). The concept of preferred directions and population vectors can also be extended to three dimensions (Georgopoulos et al., 1988) (Fig. 4B).

An extended version of this decoding scheme has been used to decode movement direction along with velocity in real-time from the spiking activity of multiple neurons recorded simultaneously in monkey motor cortex (e.g. Taylor et al., 2002; Velliste et al., 2008). Thereby, monkeys were able to learn to voluntarily control an external effector (a computer cursor in three dimensions, cf. Fig. 4C) also in the absence of arm movements and arm muscle activity. These experiments also demonstrated that this scheme generalizes over a broader space of possible directions, as the preferred directions of the cells were initially determined on the basis of activity recorded for movements to a limited number of targets but subsequently monkeys could also move the cursor to novel, untrained target positions (Taylor et al., 2002). Moreover, it has been shown that the tuning of single cells changes significantly during the acquisition of brain-control in a way that improves the control accuracy.

Similarly, MUA exhibits directional tuning and can be used to decode different aspects of arm movements (e.g. movement direction) on a single-trial basis. So far, only few publications performed a comparison of both, SUA and MUA, for the prediction of move-

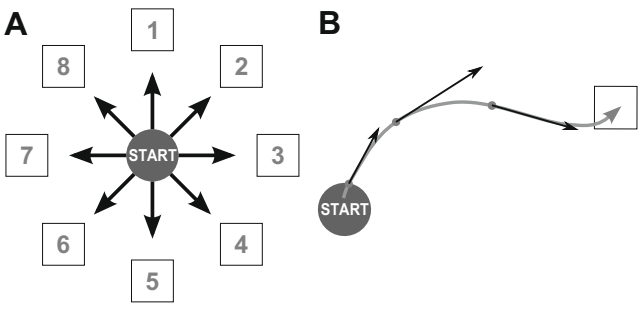

Fig. 3. Different paradigms to investigate directional tuning. (A) Center-out movements: movements (usually hand and/or arm) are performed from a central starting point to one of several targets around the origin. (B) Movement trajectories: movements are performed freely, to an arbitrary target, or as a pursuit in following a moving target. Velocity vectors and/or current position are estimated at successive times dense enough to represent the trajectory satisfyingly. Decoding then refers to a regression of continuous variables.

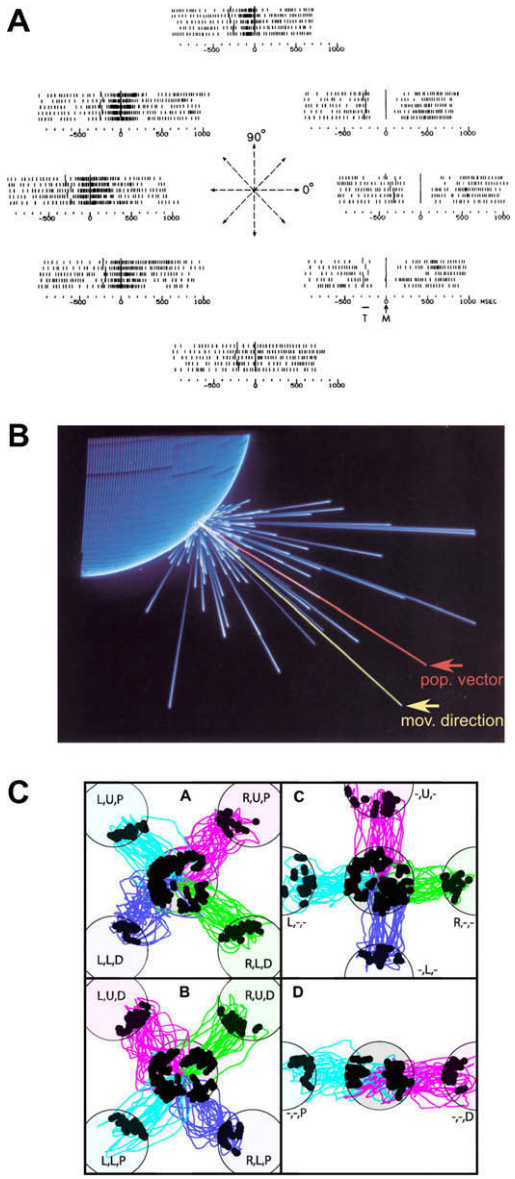

Fig. 4. Classical direct motor BMI approach based on single-unit activity (SUA) and population vector decoding. (A) From Georgopoulos et al. (1982): variation of the discharge of a motor cortical cell with different movement directions in two dimensions. For each movement direction (center) five trials (in surrounding plots) are shown, aligned to movement onset. Dashes indicate single spikes. (B) From Georgopoulos et al. (1988): example of population coding of movement direction in three dimensions. Blue lines (reflecting preferred directions of each cell scaled by firing rates) represent the vectorial contributions of individual cells in the population. The movement direction vector is shown in yellow and the direction of the population vector in red. (C) From Taylor et al. (2002). Reprinted with permission from AAAS: application of the three-dimensional population vector approach to control a prosthetic device in real-time. A monkey's brain-controlled trajectories are shown for movements from the center to one of eight targets located on the corners of a cube (trained target, subplots A and B) or for movements to one out of six untrained targets on the center points of the faces of a cube (subplots C and D).

ments (Mehring et al., 2003; Carmena et al., 2003; Stark and Abeles, 2007). Carmena et al. report that the contribution of single units (SUA) for the decoding of movement parameters in a continuous control task was about 20% higher than that of the same number of multi-units (MUA). However, they state that this difference was not critical for the maintenance of high levels of closed-loop BMI control. While Mehring et al. also report on a slight advantage of SUA over MUA in an offline analysis, Stark and Abeles found MUA (in their study called multiple spike activity instead of MUA) to be more informative about movements than SUA.

2.2. Amplitude spectrograms of analog population signals

Analog population signals (LFP, ECoG, EEG, MEG) exhibit characteristic amplitude modulations in different frequency bands during center-out movements. In Fig. 5, all spectrograms show recordings from motor cortex contra-lateral to the moved limb. Remarkably, all investigated signal types (LFP, ECoG, EEG, MEG) show a similar modulation pattern up to about 90 Hz, although the signals span a wide range of spatial resolution at which neural activity was measured (from some hundreds of micrometers up to a few centimeters).

During center-out movements, three main frequency bands can be differentiated in all investigated analog signals (frequency ranges taken from Rickert et al., 2005 (LFP); Ball et al., 2009 (ECoG); Waldert et al., 2008 (EEG/MEG)):

(a) A low frequency band (LFP: $\leqslant$13 Hz, ECoG: <2 Hz, EEG/MEG: $\leqslant$7 Hz) exhibiting a change in amplitude during the movement. In LFP this low frequency band has been further differentiated into two bands (<4 Hz and 6–13 Hz, see Rickert et al., 2005) with different temporal modulation. This band corresponds to the movement related potential (MRP) seen in the trial-averaged raw signals, which is mainly composed of slow signal components. It is highly relevant for decoding of movement direction and will be discussed in more detail later.

(b) An intermediate frequency band (LFP: 16–42 Hz, ECoG: 6–30 Hz, EEG/MEG: 10–30 Hz) showing a decrease in amplitude starting shortly before and lasting until the end of the movement. This is a well known effect accompanying movements in general and has been shown many times in different movement paradigms (e.g. EEG – Pfurtscheller, 1989; LFP – Donoghue et al., 1998; ECoG – Crone et al., 1998a; MEG – Salmelin et al., 1995). These oscillations, including mu- and beta-rhythms, are observed across large regions of the motor cortex and the presence, in particular of the mu-rhythm, is often interpreted as an idling state of motor regions, interrupted (amplitude decrease) by movement control (Pfurtscheller et al., 2003).

(c) A broad high-frequency band (LFP: 63–200 Hz, ECoG: 34–128 Hz, EEG/MEG: 62–87 Hz) showing a movement related amplitude increase consistently across all signal types. This increase in the high-gamma range has also been described in other movement studies using ECoG (Arroyo et al., 1993; Crone et al., 1998b, 2006; Pfurtscheller et al., 2003), EEG (Ball et al., 2008), and has meanwhile been corroborated for MEG (e.g. Cheyne et al., 2008). The neuro-physiological meaning and mechanisms underlying the high-gamma activity is debated (cf. Cheyne et al., 2008).

In general, it seems that non-invasive recording techniques are less capable of revealing high frequencies (Dalal et al., 2008; Waldert et al., 2008), and only few publications clearly show movement dependent very high gamma modulations above 90 Hz that are unlikely to be due to artifacts (Gonzalez et al., 2006; Ball et al., 2008). The following reasons might explain this observation: (i) Due to capacitive effects accompanying neural signal transmission along dendrites, the amplitude of extracellular field potentials decreases with increasing frequencies (Nunez and Srinivasan, 2006, pp. 189–193): disregarding active effects of ion channels, the dendritic membrane can be approximated as resistors and capacitors in a parallel circuit. The higher the frequency in such a circuit, the lower the total resistance. Thus, with increasing frequency also the

membrane leakage current increases, which effectively decreases the amount and distance (source-sink) of current flow through the dendrite and, thereby, weakens the electromagnetic fields created by this current flow. Therefore, the signal-to-noise ratio in high-frequencies might often be too weak to make high frequency signals detectable with extracranial sensors, which are more distant from the sources than LFP or ECoG electrodes. (ii) The recording situation in extracranial recordings resembles that of a spatial low-pass filter (Nunez and Srinivasan, 2006, pp. 261–273). High frequency modulations of movement related neural activity has been reported to be more focal than modulations in lower frequencies (e.g. Crone et al., 1998b; Miller et al., 2007) and might therefore be averaged into surrounding activity, when observed from outside the head. Nevertheless, it should be noted that

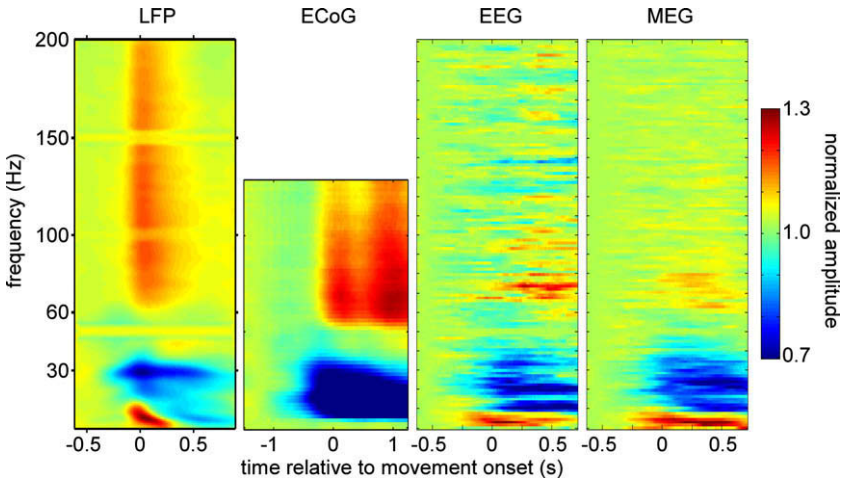

Fig. 5. Grand-average time-resolved amplitude spectrograms during center-out movements for the different recording techniques (LFP, ECoG, EEG, MEG). Spectrograms depict trial-average across all movement directions averaged across multiple subjects. Recording sites were in or above the motor cortex contra-lateral to center-out hand/arm movements. LFP recordings from motor cortex of monkeys (taken from Rickert et al. (2005)), ECoG recordings from primary motor cortex of epilepsy patients (taken from Ball et al. (2009)), EEG (re-analyzed from Waldert et al. (2008)) and MEG (taken from Waldert et al. (2008)) recorded simultaneously from motor areas from healthy subjects.

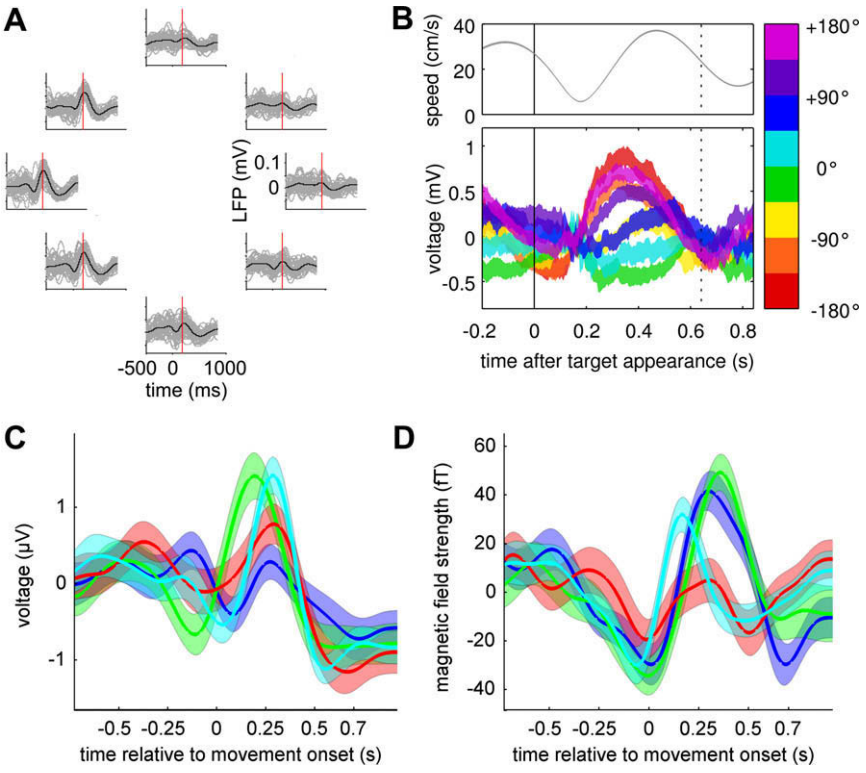

Fig. 6. Directionally tuned, low-pass filtered movement-related potentials (MRPs) in different types of population signals. (A) Trial-averaged (black) and single-trial (gray) monkey LFP for eight different directions of center-out movements, aligned on movement onset. (B) Average human ECoG from one electrode on hand/arm motor cortex, measured during continuous target-to-target movement and sorted for eight different instantaneous movement directions (lower plot). The vertical solid line shows the time of a new target appearance ($t = 0$) while the dotted line indicates the median time of target reaching. Colored bands display the mean over all single traces of one direction ± standard-error of the mean. The upper inset shows the average magnitude of hand velocity. (C) Averaged MRP recorded simultaneously with one EEG electrode and one MEG sensor (D), from Waldert et al. (2008), above the contra-lateral motor area of one subject (average ± standard-error of the mean across all trials for each direction, blue – right, green – up, red – left, cyan – down).

modulations of very high-gamma activity (up to 200 Hz) during visually cued movements were also measured non-invasively using EEG (Gonzalez et al., 2006). And during a pure motor task, it has been shown that high-gamma EEG amplitude increases up to 130 Hz can be observed around the end of a center-out arm movement (Ball et al., 2008).

2.3. Directional tuning in analog population signals: LFP, ECoG, EEG, MEG

Analysis of LFPs from monkey motor cortex showed that low-pass filtered LFP signals show directional tuning of a similar strength as the simultaneously recorded SUA and MUA signals (Mehring et al., 2003). The LFP tuning often also approximately resembled a cosine function (Rickert et al., 2005). An example of a directionally tuned MRP, derived from low-pass filtered monkey LFP during center-out movements, can be seen in Fig. 6A. Besides the low-pass filtered signals, LFP directional tuning can also be found in amplitude modulations (see Section 2.2) of different frequency bands (<4 Hz, 6–13 Hz, 63–200 Hz, Rickert et al., 2005). However, most directional information could be decoded from the low-pass filtered LFP and the amplitude modulations of the low (<4 Hz) frequency band, followed by the high (63–200 Hz) and the 6–13 Hz frequency band. While the low-pass filtered LFP is obtained by filtering in the time domain, amplitude modulations in a single frequency band only comprise (persistently positive) amplitude values, neglecting phase information of the original signal. These can be obtained from short-time Fourier transform analysis, for instance.

Directional tuning is also present in the ECoG, in the low-pass filtered signals (Mehring et al., 2004; Schalk et al., 2007; Ball et al., 2009) and in the amplitude modulations of different frequency bands (40–160 Hz – Leuthardt et al., 2004; $\leqslant$2 Hz and 34–128 Hz – Ball et al., 2009). Tuning strength is sufficient for relatively accurate directional decoding (see next section for more details) from low-pass filtered signals as well as from amplitude modulations of different frequency bands recorded simultaneously from multiple electrodes (Leuthardt et al., 2004; Ball et al., 2009). Fig. 6B shows an example of distinct directional tuning of the low-pass filtered ECoG signal measured over primary motor cortex during nonstop movements from target to target, illustrating its use for decoding of more variable, continuous hand/arm movements instead of stereotyped center-out movements.

For both non-invasive recording techniques, EEG and MEG, it has been shown that directional tuning can even be observed by measuring brain activity from outside the head (Waldert et al., 2008). Thus, directional tuning is also present in signals reflecting the activity of large neuronal populations. In contrast to LFP and ECoG, substantial directional tuning was mainly found in the low-pass filtered signals (here $\leqslant$3 Hz), nearly absent in amplitude modulations of low ($\leqslant$7 Hz), and not present in high-frequencies (62–87 Hz). Fig. 6C and D show the directionally tuned low-pass filtered signal for EEG and MEG, respectively, as recorded simultaneously with electrodes/sensors above contra-lateral motor cortex in one subject.

3. Movement decoding

3.1. Movement decoding using analog population signals: movement direction

Directional tuning, as found in each recording technique from SUA to EEG/MEG, may be utilized for directional decoding in a direct motor BMI. As described above, either the firing rates of single neurons (SUA) or, for analog signals, the low-pass filtered activity and spectral amplitude modulations can be used as input to a decoder.

Decoding performance can be quantified via decoding accuracy (*DA*), defined as the percentage of correctly decoded trials, or decoded information (*DI*), which quantifies the amount of information extracted about movement direction. The *DI* is defined as Shannon's mutual information (Cover and Thomas, 1991) between decoded and real movement direction:

$$DI(t_d,t_r)=\sum_{t_d\in T_d}\sum_{t_r\in T_r}p(t_d,t_r)\cdot\log_2\frac{p(t_d,t_r)}{p(t_d)\cdot p(t_r)} \quad (1)$$

where T_d and T_r are sets of decoded and real targets (movement directions), $p(t_d)$ and $p(t_r)$ the marginal probability distributions of decoded and real targets, and $p(t_d,t_r)$ the joint probability distribution of decoded and real targets, respectively. Under the assumptions of equal probabilities for correct predictions for each direction and equal distributions of false predictions across directions, the following relation of *DI* and *DA* can be derived (Waldert et al., 2008):

$$DI(DA)=\frac{DA}{100}\cdot\log_2\frac{DA}{DA_{chance}}+\frac{100-DA}{100}\cdot\log_2\frac{100-DA}{100-DA_{chance}} \quad (2)$$

where *DA* is the percentage of correctly decoded directions and DA_{chance} the decoding accuracy expected by chance.

The performance measure *DI* allows, in contrast to *DA*, to directly compare the decoding performance achieved in studies using different numbers of targets. Both measures are used in Fig. 7 to visualize and compare the decoding performances achieved using recording techniques from SUA to EEG/MEG in similar center-out experiments with three to eight targets. SUA, MUA, and LFP signals from 48 electrodes (implanted in the motor cortices of both hemispheres) show substantially higher decoding performances than the extracortical recordings. On the next level, plotting *DI* values allows one to see that the invasive ECoG pro-

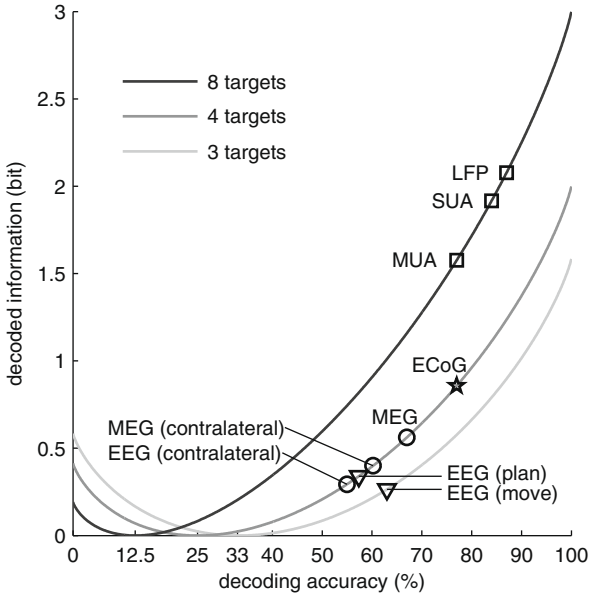

Fig. 7. Comparison of different recording techniques with respect to the decoding accuracy (*DA*) and the decoded information (*DI*) about movement direction for center-out experiments. The gray curves reflect the dependency of *DI* on *DA* under certain simplifying assumptions (Eq. (2), Section 3.1) for 3, 4, or 8 targets. (squares – Mehring et al., 2003; star – Ball et al., 2009; circles – Waldert et al., 2008 (contralateral: only sensors above contra-lateral motor areas were used, otherwise sensors above contra- and ipsilateral motor areas were used); triangles – Hammon et al., 2008 (plan/move refers to decoding of brain activity during planning/movement phase)).

vides up to twice as much decoded information about movement direction than non-invasive EEG and MEG, which are similar in terms of decoding performance. In addition to findings from our group (Waldert et al., 2008), directional decoding in EEG has also been corroborated by Hammon et al. (2008), showing that the target location during reach (one out of three targets) and during planning period before reach (one out of four targets) can be inferred.

The following points must be noted to interpret this comparison: (i) The decoding performance of LFP and ECoG is dependent on the location of the implanted electrodes, the number of electrodes, and the inter-electrode distance. It might also depend on electrode size and impedance. For current ECoG implantations in epilepsy patients, these parameters are determined by the requirements of the pre-neurosurgical evaluations. An ECoG grid optimized for decoding, placed at the optimal location on the cortical surface might yield a higher decoding performance. Also the decoding performance of SUA/MUA depends on the location of the implanted electrodes and the number of extracted spike trains. (ii) Correlations in particular between neighboring EEG/MEG channels can be high. Consequently, EEG/MEG channels can exhibit a substantial degree of redundancy, thereby limiting the possible information increase gained by using additional sensors. In contrast, the decoding performance for SUA/MUA – and to a lesser extent also for LFP and ECoG – might be increased by using additional recording sites due to weaker inter-channel correlations than in EEG/MEG and, thus, less redundancy between channels.

However, it should be noted that also the measure *DI* does not allow to neglect all differences in experimental design of BMI studies in general (online vs. offline analysis, which limbs were moved, movement amplitude and speed, temporal movement constraints, definition of successful trials, etc.). While a higher number of possible targets increases the maximal amount of transferable information, it simultaneously can reduce decoding accuracy. As of now, it is difficult to judge which number of targets is optimal to achieve a maximum of decoded information.

In summary, these considerations underpin the superiority of invasive and, in particular, SUA/MUA/LFP recordings with regard to decoding performance.

3.2. Movement decoding using analog population signals: movement trajectories

Different methods for decoding of movement trajectories (see Fig. 3B) have been proposed e.g. a simple linear filter (Wessberg et al., 2000; Serruya et al., 2002; Mehring et al., 2003; Carmena et al., 2003), support-vector regression (Chang and Lin, 2002; Mehring et al., 2003; Stark and Abeles, 2007), or Kalman filters (Wu et al., 2002, 2006; Pistohl et al., 2008). Even if these techniques do not return movement direction as a discrete variable, this information is contained in estimates of the velocity vector i.e., in estimates of velocities in two or three dimensional space.

In case of decoding continuous variables, decoding performance can be quantified by the correlation or the squared correlation coefficient (Pearson correlation coefficient) between the measured, real movement trajectory and the trajectory predicted from neural activity. In the following, we will use the non-squared correlation coefficient.

Very accurate trajectory decoding has been achieved by decoding SUA: Wu et al. (2006) used a Kalman filter in order to predict movements in a continuous target-to-target task from 42 single units simultaneously recorded in monkey primary motor cortex. They obtained average correlation coefficients of 0.88 for hand position. So far, the highest decoding performance obtained from analog signal types was lower. Mehring et al. (2003) report average correlation coefficients of almost 0.7 for decoding of LFPs in monkey experiments with center-out movements. Recordings were done with eight electrodes in the motor cortices of both hemispheres and decoding used support-vector regression.

Schalk et al. (2007) investigated the prediction of two-dimensional trajectories from ECoG signals during a slow, two-dimensional, circular, continuous tracking task. Different signal components i.e., low-pass filtered signals and amplitude modulations of different frequency bands, were investigated. The low-pass filtered signal yielded the most accurate movement predictions. The average correlation coefficient obtained for position was about 0.5. Another ECoG study in humans (Pistohl et al., 2008) predicted hand trajectories in a continuous sequence of two-dimensional movements to random targets, similar to the experimental paradigm of Wu et al. Using a Kalman filter, the predictions yielded an average correlation coefficient of about 0.4, again obtained from low-pass filtered signals recorded with electrodes over contra-lateral motor cortex.

Offline decoding of continuous trajectories from (non-invasive) MEG has been demonstrated with rather high decoding performance by Georgopoulos et al. (2005) in stereotyped copying of a pentagon and by Bradberry et al. (2008) for center-out movements in combination with visuo-motor transformations.

The aforementioned findings for trajectory decoding and directional decoding (Fig. 7) demonstrate the superiority of invasive recordings for the development of a direct motor BMI in terms of decoding performance. Nevertheless, the findings also demonstrate that the clinically favorable non-invasive recording techniques could be applied. The ECoG recorded with electrodes not penetrating the cortical tissue might also be an interesting alternative being less invasive (extracortical) but still containing a high amount of information about movements. Forthcoming small, flexible, and dense micro-ECoG electrode grids could improve the information content of those signals, so far recorded with macro-ECoG electrodes designed for diagnostic purposes.

4. Discussion

4.1. Relevance of low-pass filtered analog neural population signals

The substantial information about movement kinematics in low-pass filtered neural activity has now been shown for a wide range of analog recording techniques. As a stand-alone feature, this activity always provided the highest decoding performance and might reflect a general feature of neuronal population signals as corroborated for LFP (Mehring et al., 2003; Rickert et al., 2005), ECoG (Schalk et al., 2007; Pistohl et al., 2008; Ball et al., 2009), EEG (Waldert et al., 2008), and MEG (Jerbi et al., 2007; Waldert et al., 2008; Bradberry et al., 2008). However, the decoding performance of different EEG signal features has not been systematically compared.

The directionally sensitive MRP, as it is observed by averaging the analog field potentials over multiple trials, is mostly composed of low-frequency activity. This could either mean that high-frequency activity is not well phase-locked to the movement or that the available triggers (e.g. movement onset or onset of EMG activity) lack the temporal precision to reveal phase-locked activity of fast signal components after averaging. On a descriptive level, the premovement part of the MRP might be related to the readiness potential (Kornhuber and Deecke, 1965; Brunia and Van Boxtel, 2000), a term mostly used for self-paced but also for paced movements (Rockstroh et al., 1989). For the readiness potential, considerable variation depending on parameters of the movement has previously been shown (cf. Birbaumer et al., 1990). The whole MRP might be directionally modulated in a similar way. Thus, low-pass filtering in a single-trial approach might retain

the essential signal components that make up the MRP, while eliminating noise.

Decoding of amplitude modulations (disregarding the phase) did provide directional information in LFP, ECoG, and EEG/MEG. However, in ECoG, the achieved decoding accuracy was lower than that achieved with low-pass filtered activity and in EEG/MEG it was almost at chance level (though significant).

4.2. Directional tuning of signals reflecting a wide range of spatial scales: from SUA to EEG/MEG

How could the directional tuning of neural population signals be generated? Directional tuning of single motor cortical neurons is often modeled as a cosine whose maximum defines the neuron's preferred direction (Georgopoulos et al., 1982). If we assume that neural population signals reflect a weighted summed activity of neighboring neurons, is then a spatial organization of preferred directions of single units in the motor cortex required for directional tuning of population signals or can directional tuning of population activity also arise from a random arrangement of preferred directions? To address this question, we consider the predictions of the following parsimonious model – similar models were used in Rickert (2004) and also proposed for the reconstruction of orientation and ocular dominance maps in the visual cortex from filtered white noise (Rojer and Schwartz, 1990). Recordings of population signals are viewed as the application of a spatial low-pass filter over single sources (e.g. single neurons or small clusters of neurons exhibiting similar tuning). The resulting tuning of a population signal is then a (weighted) sum of the individual cosine tuning curves. Since the sum over an arbitrary number of cosines with random phase is still a cosine (Fourier theorem), the tuning properties would persist for every kind of population signal independent of the width of the spatial low-pass filter. With N being the number of sources contributing to the spatially filtered signal and assuming, without loss of generality, equal amplitudes of cosine tuning curves, the magnitude of the resulting tuning curve will be the amplitude of the original tuning curves multiplied by $\sqrt{N}$ (see Appendix for a deduction). However, due to the fact that the trial-by-trial variability is also increased by a factor of $\sqrt{N}$ (uncorrelated noise, see Appendix for a deduction), the signal-to-noise ratio of the population signal is equal to the signal-to-noise ratio of the sources. These model considerations indicate that directional tuning of population signals might also arise in the absence of any spatial organization of preferred directions of single neurons. It also demonstrates that using population activity (MUA, LFP, ECoG, EEG, and MEG) instead of single units does not necessarily coincide with a lower signal-to-noise ratio. However, the following limitations of the model should be taken into account: (1) The modeling of analog neural populations signals as a (weighted) sum of single neuron activity might be oversimplified as these signals might also reflect e.g. inputs to the cortical area and/or synchronous activity of the neural network surrounding the recording electrodes. (2) The model ignores any spatial organization of preferred directions in the motor cortex. In fact, neurons exhibiting similar preferred directions can cluster in minicolumns of approx. 30 μm width (Georgopoulos et al., 2007). Two or three of these minicolumns with similar preferred directions tend to cluster and are repeated at a distance of approximately 240 μm (Amirikian and Georgopoulos, 2003; Georgopoulos et al., 2007). Besides this short-range order of preferred directions, no spatial organization on a larger scale has been reported so far; rather, preferred directions are widely distributed over the arm area of the primary motor cortex (Naselaris et al., 2006). (3) The model assumes cosine tuning even though also other tuning curves were observed for single neurons (Amirikian and Georgopoulos, 2000). (4) The amplitudes of tuning curves decrease more and more with source-sensor distance. Hence, the amount and the influence of external confounding noise might be increased which is not taken into account in the model. (5) The neuronal variability/noise can – other than assumed by the model – indeed, be correlated. In this case, the trial-by-trial variability of a population signal can be increased by a larger factor than for uncorrelated noise (see Appendix) and, thus, the signal-to-noise ratio of the population signal decreases.

While this model could explain the tuning in neural population signals without any spatial organization of preferred directions, one or multiple of the above limitations might also explain why the tuning strength of population signals is in fact weaker than the tuning strength of single neurons (see Figs. 6C and D, 7).

4.3. Online direct motor BMI and adaptivity

While SUA recordings have been successfully used to implement an online direct motor BMI (Serruya et al., 2002; Taylor et al., 2002; Carmena et al., 2003; Hochberg et al., 2006; Velliste et al., 2008), this has yet to be demonstrated for analog population signals. Despite the aforementioned encouraging findings, it is not clear which level of decoding performance is needed to succeed with the direct motor BMI approach in an online application.

The performance of direct motor BMIs utilizing directional tuning in SUA improves during its use and can finally reach very high levels. One important reason for this improvement are changes in the cells' tuning properties i.e., the tuning of the firing rate becomes more pronounced (Taylor et al., 2002; Carmena et al., 2003) and more cosine-like (Taylor et al., 2002) and, thus, allows for more accurate decoding. Whether the decoding performance in direct motor BMIs based on epicortical or extracranial recordings can also increase during the acquisition of brain-control is currently unknown. For SUA, only the activity of single neurons must be adapted. It might be possible that neural mass activity can also be tuned or shaped via BMI training and, eventually, yield a substantial increase in decoding performance. This adaptivity on the side of the brain should then be additionally combined with adaptive decoding algorithms (Taylor et al., 2002; Li and Guan, 2006; Shenoy et al., 2006; Vidaurre et al., 2006; Blumberg et al., 2007; Wu and Hatsopoulos, 2008) on the machine side. Such co-adaptive approaches might ultimately yield the highest decoding performance and, thus, facilitate BMI usability.

Acknowledgments

This work was partially supported by the German Federal Ministry of Education, research grants 01GQ0420, 01GQ0761 TP 1, 0313891, and a scholarship from the German National Academic Foundation, and the German Research Foundation, grant 550/C6. We thank Andreas Schulze-Bonhage for collaborating on the ECoG experiments (Pistohl et al., 2008) re-analyzed in this study. We thank Hubert Preissl and Niels Birbaumer for the collaboration on the MEG/EEG experiments (Waldert et al., 2008) re-analyzed in this study. We thank Evariste Demandt for discussions on this manuscript.

Appendix A

A.1. Deduction of the expected amplitude of a cosine created by the sum of cosines with random phases

We consider N cosines of frequency one, phase α_i, and amplitude c_i. The Fourier theorem predicts for their sum:

$$a \cdot \cos(\varphi + \gamma) = \sum_{i=1}^{N} c_i \cdot \cos(\varphi + \alpha_i) \tag{A1}$$

With γ being the resulting phase and a the resulting amplitude. Based on trigonometric functions, this equation can be transformed as follows:

$$a\cdot[\cos(\varphi)\cdot\cos(\gamma)-\sin(\varphi)\cdot\sin(\gamma)]=\sum_{i=1}^{N}c_i\cdot[\cos(\varphi)\cdot\cos(\alpha_i)-\sin(\varphi)\cdot\sin(\alpha_i)]$$

$$a\cdot\cos(\varphi)\cdot\cos(\gamma)-a\cdot\sin(\varphi)\cdot\sin(\gamma)=\sum_{i=1}^{N}c_i\cdot\cos(\varphi)\cdot\cos(\alpha_i)-\sum_{i=1}^{N}c_i\cdot\sin(\varphi)\cdot\sin(\alpha_i)$$

$$\cos(\varphi)\cdot a\cdot\cos(\gamma)-\sin(\varphi)\cdot a\cdot\sin(\gamma)=\cos(\varphi)\cdot\sum_{i=1}^{N}c_i\cdot\cos(\alpha_i)-\sin(\varphi)\cdot\sum_{i=1}^{N}c_i\cdot\sin(\alpha_i)$$

$$a\cdot\cos(\gamma)=\sum_{i=1}^{N}c_i\cdot\cos(\alpha_i)\Rightarrow[a\cdot\cos(\gamma)]^2=\left(\sum_{i=1}^{N}c_i\cdot\cos(\alpha_i)\right)^2$$

$$a\cdot\sin(\gamma)=\sum_{i=1}^{N}c_i\cdot\sin(\alpha_i)\Rightarrow[a\cdot\sin(\gamma)]^2=\left(\sum_{i=1}^{N}c_i\cdot\sin(\alpha_i)\right)^2$$

$$[a\cdot\cos(\gamma)]^2+[a\cdot\sin(\gamma)]^2=\left(\sum_{i=1}^{N}c_i\cdot\cos(\alpha_i)\right)^2+\left(\sum_{i=1}^{N}c_i\cdot\sin(\alpha_i)\right)^2$$

$$\begin{aligned}a^2\cdot\left[\cos^2(\gamma)+\sin^2(\gamma)\right]&=c_1^2\cdot\cos^2(\alpha_1)+c_1^2\cdot\sin^2(\alpha_1)+\ldots\\&\quad+c_N^2\cdot\cos^2(\alpha_N)+c_N^2\cdot\sin^2(\alpha_N)\\&\quad+2\cdot c_1\cdot c_2\cdot\cos(\alpha_1)\cdot\cos(\alpha_2)\\&\quad+2\cdot c_1\cdot c_2\cdot\sin(\alpha_1)\cdot\sin(\alpha_2)+\ldots\\&\quad+2\cdot c_{N-1}\cdot c_N\cdot\cos(\alpha_{N-1})\cdot\cos(\alpha_N)\\&\quad+2\cdot c_{N-1}\cdot c_N\cdot\sin(\alpha_{N-1})\cdot\sin(\alpha_N)\end{aligned}$$

$$\begin{aligned}a^2\cdot\underbrace{[\cos^2(\gamma)+\sin^2(\gamma)]}_{=1}&=c_1^2\cdot[\cos^2(\alpha_1)+\sin^2(\alpha_1)]+\ldots+c_N^2\cdot[\cos^2(\alpha_N)+\sin^2(\alpha_N)]\\&\quad+2\cdot c_1\cdot c_2\cdot[\cos(\alpha_1)\cdot\cos(\alpha_2)+\sin(\alpha_1)\cdot\sin(\alpha_2)]+\ldots\\&\quad+2\cdot c_{N-1}\cdot c_N\cdot\underbrace{[\cos(\alpha_{N-1})\cdot\cos(\alpha_N)+\sin(\alpha_{N-1})\cdot\sin(\alpha_N)]}_{\cos(\alpha_{N-1}-\alpha_N)}\end{aligned}$$

$$a^2=\sum_{i=1}^{N}(c_i^2)+2\cdot c_1\cdot c_2\cdot cos(\alpha_1-\alpha_2)+\ldots+2\cdot c_{N-1}\cdot c_N\cdot\cos(\alpha_{N-1}-\alpha_N)$$

$$a^2=\sum_{i=1}^{N}c_i^2+2\cdot\sum_{i,j}^{N}c_i\cdot c_j\cdot\cos(\alpha_i-\alpha_j)\quad\forall i\neq j$$

$$a=\sqrt{\sum_{i=1}^{N}c_i^2+2\cdot\sum_{i,j}^{N}c_i\cdot c_j\cdot\cos(\alpha_i-\alpha_j)}\quad\forall i\neq j$$

With α uniformly distributed i.e., $PDF(\alpha)=\begin{pmatrix}\frac{1}{2\pi} & \text{for} & 0\leqslant\alpha<2\pi\\ 0 & \text{else}\end{pmatrix}$

$$\langle a\rangle=\sqrt{\sum_{i=1}^{N}c_i^2}\tag{A2}$$

With equal amplitudes $c_i=C=const.\ \forall i$ of the original cosines, this yields:

$$\langle a\rangle=\sqrt{\sum_{i=1}^{N}C^2}=C\cdot\sqrt{N}\tag{A3}$$

A.2. Deduction of the noise amplitude resulting from summation of noise

We consider a signal y that is created by summing up N noise sources x_i.

$$y=f(x_1,x_2,\ldots,x_N)=\sum_{i=1}^{N}x_i$$

The variance σ_f^2 of the noise y can be calculated by Gaussian error propagation:

$$\sigma_f^2=\sum_{i=1}^{N}\left(\frac{\partial f}{\partial x_i}\right)^2\sigma_{x_i}^2+\sum_{i=1}^{N}\sum_{i\neq j}^{N}\left(\frac{\delta f}{\delta x_i}\frac{\delta f}{\delta x_j}\right)\cdot Cov(x_i,x_j)\tag{A4}$$

For independent noise sources, the second term reduces to zero and, due to f being a sum, the following holds for the first term:

$$\frac{\partial f}{\partial x_i}=1\ \forall i,\ \text{therefore}$$

$$\sigma_f=\sqrt{\sigma_{x_1}^2+\sigma_{x_2}^2+\ldots+\sigma_{x_N}^2}$$

With $\sigma_{x_i}=\sigma=const.\ \forall i$

$$\sigma_f=\sqrt{N}\cdot\sigma\tag{A5}$$

However, for correlated noise sources, the variance of the noise y can be higher because the second term in Eq. (A4) can be nonzero.

References

Allison, B.Z., McFarland, D.J., Schalk, G., Zheng, S.D., Jackson, M.M., Wolpaw, J.R., 2008. Towards an independent brain-computer interface using steady state visual evoked potentials. Clin. Neurophysiol. 119 (2), 399–408.

Amirikian, B., Georgopoulos, A.P., 2000. Directional tuning profiles of motor cortical cells. Neurosci. Res. 36 (1), 73–79.

Amirikian, B., Georgopoulos, A.P., 2003. Modular organization of directionally tuned cells in the motor cortex: is there a short-range order? Proc. Natl. Acad. Sci. 100 (21), 12474–12479.

Arroyo, S., Lesser, R.P., Gordon, B., Uematsu, S., Jackson, D., Webber, R., 1993. Functional significance of the mu rhythm of human cortex: an electrophysiologic study with subdural electrodes. Electroencephalogr. Clin. Neurophysiol. 87 (3), 76–87.

Ball, T., Demandt, E., Mutschler, I., Neitzel, E., Mehring, C., Vogt, K., Aertsen, A., Schulze-Bonhage, A., 2008. Movement related activity in the high gamma range of the human EEG. Neuroimage 41 (2), 302–310.

Ball, T., Schulze-Bonhage, A., Aertsen, A., Mehring, C., 2009. Differential representation of arm movement direction in relation to cortical anatomy and function. J. Neural. Eng. 6 (1), 016006.

Birbaumer, N., Elbert, T., Canavan, A.G., Rockstroh, B., 1990. Slow potentials of the cerebral cortex and behavior. Physiol. Rev. 70 (1), 1–41.

Birbaumer, N., Ghanayim, N., Hinterberger, T., Iversen, I., Kotchoubey, B., Kübler, A., Perelmouter, J., Taub, E., Flor, H., 1999. A spelling device for the paralysed. Nature 398 (6725), 297–298.

Blankertz, B., Dornhege, G., Krauledat, M., Müller, K.R., Curio, G., 2007. The non-invasive Berlin brain-computer interface: fast acquisition of effective performance in untrained subjects. Neuroimage 37 (2), 539–550.

Blumberg, J., Rickert, J., Waldert, S., Schulze-Bonhage, A., Aertsen, A., Mehring, C., 2007. Adaptive classification for brain computer interfaces. In: Proc. of Int. Conf. IEEE Engineering in Medicine and Biology.

Bradberry, T.J., Contreras-Vidal, J.L., Rong, F., 2008. Decoding hand and cursor kinematics from magnetoencephalographic signals during tool use. In: IEEE-EMBS, Conf. Proc. pp. 5306–5309.

Brunia, K., Van Boxtel, G., 2000. Motor preparation. In: Caccioppo, J.T., Tassinary, L., Bertson, G. (Eds.), Handbook of Psychophysiology, 2nd ed. Cambridge Univ.Press, pp. 507–533.

Carmena, J.M., Lebedev, M.A., Crist, R.E., O'Doherty, J.E., Santucci, D.M., Dimitrov, D.F., Patil, P.G., Henriquez, C.S., Nicolelis, M.A., 2003. Learning to control a brain-machine interface for reaching and grasping by primates. PLoS Biol. 1 (2), E42.

Chang, C.C., Lin, C.J., 2002. Training ν-support vector regression: theory and algorithms. Neural Comput. 14 (8), 1959–1977.

Cheyne, D., Bells, S., Ferrari, P., Gaetz, W., Bostan, A.C., 2008. Self-paced movements induce high-frequency gamma oscillations in primary motor cortex. Neuroimage 42 (1), 332–342.

Cover, T.M., Thomas, J.A., 1991. Elements of Information Theory. John Wiley & Sons Inc..

Crone, N.E., Miglioretti, D.L., Gordon, B., Sieracki, J.M., Wilson, M.T., Uematsu, S., Lesser, R.P., 1998a. Functional mapping of human sensorimotor cortex with electrocorticographic spectral analysis. I. Alpha and beta event-related desynchronization. Brain 121, 2271–2299.

Crone, N.E., Miglioretti, D.L., Gordon, B., Lesser, R.P., 1998b. Functional mapping of human sensorimotor cortex with electrocorticographic spectral analysis. II. Event-related synchronization in the gamma band. Brain 121, 2301–2315.

Crone, N.E., Sinai, A., Korzeniewska, A., 2006. High-frequency gamma oscillations and human brain mapping with electrocorticography. Prog. Brain Res. 159, 275–295.

Curran, E., Sykacek, P., Stokes, M., Roberts, S.J., Penny, W., Johnsrude, I., Owen, A.M., 2004. Cognitive tasks for driving a brain-computer interfacing system: a pilot study. IEEE Trans. Neural. Syst. Rehabil. Eng. 12 (1), 48–54.

Dalal, S.S., Guggisberg, A.G., Edwards, E., Sekihara, K., Findlay, A.M., Canolty, R.T., Berger, M.S., Knight, R.T., Barbaro, N.M., Kirsch, H.E., Nagarajan, S.S., 2008. Five-dimensional neuroimaging: localization of the time-frequency dynamics of cortical activity. Neuroimage 40 (4), 1686–1700.

Donoghue, J.P., Sanes, J.N., Hatsopoulos, N.G., Gaal, G., 1998. Neural discharge and local field potential oscillations in primate motor cortex during voluntary movements. J. Neurophysiol. 79 (1), 159–173.

Farwell, L.A., Donchin, E., 1988. Talking off the top of your head: toward a mental prosthesis utilizing event-related brain potentials. Electroencephalogr. Clin. Neurophysiol. 70 (6), 510–523.

Georgopoulos, A.P., Kalaska, J.F., Caminiti, R., Massey, J.T., 1982. On the relations between the direction of two-dimensional arm movements and cell discharge in primate motor cortex. J. Neurosci. 2 (11), 1527–1537.

Georgopoulos, A.P., Caminiti, R., Kalaska, J.F., Massey, J.T., 1983. Spatial coding of movement: a hypothesis concerning the coding of movement direction by motor cortical populations. Exp. Brain Res. Supplement 7, 327–336.

Georgopoulos, A.P., Schwartz, A.B., Kettner, R.E., 1986. Neuronal population coding of movement direction. Science 233 (4771), 1416–1419.

Georgopoulos, A.P., Kettner, R.E., Schwartz, A.B., 1988. Primate motor cortex and free arm movements to visual targets in three-dimensional space. II. Coding of the direction of movement by a neuronal population. J. Neurosci. 8 (8), 2928–2937.

Georgopoulos, A.P., Langheim, F.J.P., Leuthold, A.C., Merkle, A.N., 2005. Magnetoencephalographic signals predict movement trajectory in space. Exp. Brain Res. 25, 132–135.

Georgopoulos, A.P., Merchant, H., Naselaris, T., Amirikian, B., 2007. Mapping of the preferred direction in the motor cortex. Proc. Natl. Acad. Sci. 104 (26), 11068–11072.

Gonzalez, S.L., Grave de Peralta, R., Thut, G., Millán, J.d.R., Morier, P., Landis, T., 2006. Very high frequency oscillations (VHFO) as a predictor of movement intentions. Neuroimage 32 (1), 170–179.

Hammon, P.S., Makeig, S., Poizner, H., Todorov, E., de Sa, V.R., 2008. Predicting reaching targets from human EEG. IEEE Signal Proc Mag 25 (1), 69–77.

Hochberg, L.R., Serruya, M.D., Friehs, G.M., Mukand, J.A., Saleh, M., Caplan, A.H., Branner, A., Chen, D., Penn, R.D., Donoghue, J.P., 2006. Neuronal ensemble control of prosthetic devices by a human with tetraplegia. Nature 442, 164–171.

Hoffmann, U., Vesin, J.M., Ebrahimi, T., Diserens, K., 2008. An efficient P300-based brain-computer interface for disabled subjects. J. Neurosci. Methods 167 (1), 115–125.

Jerbi, K., Lachaux, J.P., N'Diaye, K., Pantazis, D., Leahy, R.M., Garnero, L., Baillet, S., 2007. Coherent neural representation of hand speed in humans revealed by MEG imaging. Proc. Natl. Acad. Sci. 104 (18), 7676–7681.

Kennedy, P.R., Bakay, R.A., 1998. Restoration of neural output from a paralyzed patient by a direct brain connection. Neuroreport 9 (8), 1707–1711.

Kornhuber, H.H., Deecke, L., 1965. Changes in the brain potential in voluntary movements and passive movements in man: readiness potential and reafferent potentials. Pflugers Arch Gesamte Physiol Menschen Tiere 10 (284), 1–17.

Leuthardt, E.C., Schalk, G., Wolpaw, J.R., Ojemann, J.G., Moran, D.W., 2004. A brain-computer interface using electrocorticographic signals in humans. J. Neural Eng. 1 (2), 63–71.

Li, Y., Guan, C., 2006. An extended EM algorithm for joint feature extraction and classification in brain-computer interfaces. Neural Comput. 18 (11), 2730–2761.

McFarland, D.J., Krusienski, D.J., Sarnacki, W.A., Wolpaw, J.R., 2008. Emulation of computer mouse control with a noninvasive brain–computer interface. J. Neural Eng. 5 (2), 101–110.

Mehring, C., Rickert, J., Vaadia, E., de Oliveira, S.C., Aertsen, A., Rotter, S., 2003. Inference of hand movements from local field potentials in monkey motor cortex. Nat. Neurosci. 6 (12), 1253–1254.

Mehring, C., Nawrot, M.P., de Oliveira, S.C., Vaadia, E., Schulze-Bonhage, A., Aertsen, A., Ball, T., 2004. Comparing information about arm movement direction in single channels of local and epicortical field potentials from monkey and human motor cortex. J. Physiol. Paris 98 (4–6), 498–506.

Middendorf, M., McMillan, G., Calhoun, G., Jones, K.S., 2000. Brain-computer interfaces based on the steady-state visual-evoked response. IEEE Trans. Rehabil. Eng. 8 (2), 211–213.

Miller, K.J., denNijs, M., Shenoy, P., Miller, J.W., Rao, R.P., Ojemann, J.G., 2007. Real-time functional brain mapping using electrocorticography. Neuroimage 37 (2), 504–507.

Moran, D.W., Schwartz, A.B., 1999. Motor cortical representation of speed and direction during reaching. J. Neurophysiol. 82 (5), 2676–2692.

Naselaris, T., Merchant, H., Amirikian, B., Georgopoulos, A.P., 2006. Large-scale organization of preferred directions in the motor cortex. II. Analysis of local distributions. J. Neurophysiol. 96 (6), 3237–3247.

Nunez, P.L., Srinivasan, R., 2006. Electric Fields of the Brain, 2nd ed. Oxford University Press, Inc..

Penny, W.D., Roberts, S.J., 1999. EEG-based communication via dynamic neural network models. In: International Joint Conference on Neural Networks (IJCNN).

Pfurtscheller, G., 1989. Functional topography during sensorimotor activation studied with event-related desynchronization mapping. J. Clin. Neurophysiol. 6 (1), 75–84.

Pfurtscheller, G., Flotzinger, D., Kalcher, J., 1993. Brain-Computer Interface–a new communication device for handicapped persons. J. Microcomp. Appl. 16, 293–299.

Pfurtscheller, G., Graimann, B., Huggins, J.E., Levine, S.P., Schuh, L.A., 2003. Spatiotemporal patterns of beta desynchronization and gamma synchronization in corticographic data during self-paced movement. Clin. Neurophysiol. 114 (7), 1226–1236.

Pfurtscheller, G., Neuper, C., 2006. Future prospects of ERD/ERS in the context of brain-computer interface (BCI) developments. Prog. Brain Res. 159, 433–437.

Pistohl, T., Ball, T., Schulze-Bonhage, A., Aertsen, A., Mehring, C., 2008. Prediction of arm movement trajectories from ECoG-recordings in humans. J. Neurosci. Methods 167 (1), 105–115.

Rickert, J., 2004. Representation of movement direction in the motor cortex. Ph.D. Thesis, Albert-Ludwigs-University, Freiburg, Germany.

Rickert, J., de Oliveira, S.C., Vaadia, E., Aertsen, A., Rotter, S., Mehring, C., 2005. Encoding of movement direction in different frequency ranges of motor cortical local field potentials. J. Neurosci. 25 (39), 8815–8824.

Rockstroh, B., Elbert, T., Canavan, A., Lutzenberger, W., Birbaumer, N., 1989. Slow Cortical Potentials and Behaviour, 2nd ed. Urban, Baltimore.

Rojer, A.S., Schwartz, E.L., 1990. Cat and monkey cortical columnar patterns modeled by bandpass-filtered 2D white noise. Biol. Cybern. 62 (5), 381–391.

Salmelin, R., Hämäläinen, M., Kajola, M., Hari, R., 1995. Functional segregation of movement-related rhythmic activity in the human brain. Neuroimage 2 (4), 237–243.

Schalk, G., Kubánek, J., Miller, K.J., Anderson, N.R., Leuthardt, E.C., Ojemann, J.G., Limbrick, D., Moran, D., Gerhardt, L.A., Wolpaw, J.R., 2007. Decoding two-dimensional movement trajectories using electrocorticographic signals in humans. J. Neural Eng. 4, 264–275.

Sellers, E.W., Kübler, A., Donchin, E., 2006. Brain-computer interface research at the University of South Florida cognitive psychophysiology laboratory: the P300 speller. IEEE Trans. Neural Syst. Rehabil. Eng. 14 (2), 221–224.

Serruya, M.D., Hatsopoulos, N.G., Paninski, L., Fellows, M.R., Donoghue, J.P., 2002. Instant neural control of a movement signal. Nature 416 (6877), 141–142.

Shenoy, P., Krauledat, M., Blankertz, B., Rao, R.P., Müller, K.R., 2006. Towards adaptive classification for BCI. J. Neural Eng. 3 (1), R13–23.

Sitaram, R., Zhang, H., Guan, C., Thulasidas, M., Hoshi, Y., Ishikawa, A., Shimizu, K., Birbaumer, N., 2007. Temporal classification of multichannel near-infrared spectroscopy signals of motor imagery for developing a brain–computer interface. Neuroimage 34 (4), 1416–1427.

Stark, E., Abeles, M., 2007. Predicting movement from multiunit activity. J. Neurosci. 27 (31), 8387–8394.

Taylor, D.M., Tillery, S.I., Schwartz, A.B., 2002. Direct cortical control of 3D neuroprosthetic devices. Science 296 (5574), 1829–1832.

Vidaurre, C., Schlögl, A., Cabeza, R., Scherer, R., Pfurtscheller, G., 2006. A fully on-line adaptive BCI. IEEE Trans. Biomed. Eng. 53 (6), 1214–1219.

Velliste, M., Perel, S., Spalding, M.C., Whitford, A.S., Schwartz, A.B., 2008. Cortical control of a prosthetic arm for self-feeding. Nature 453 (7198), 1098–1101.

Waldert, S., Preissl, H., Demandt, E., Braun, C., Birbaumer, N., Aertsen, A., Mehring, C., 2008. Hand movement direction decoded from MEG and EEG. J. Neurosci. 28 (4), 1000–1008.

Wessberg, J., Stambaugh, C.R., Kralik, J.D., Beck, P.D., Laubach, M., Chapin, J.K., Kim, J., Biggs, S.J., Srinivasan, M.A., Nicolelis, M.A.L., 2000. Real-time prediction of hand trajectory by ensembles of cortical neurons in primates. Nature 408 (6810), 361–365.

Wolpaw, J.R., McFarland, D.J., Neat, G.W., Forneris, C.A., 1991. An EEG-based brain-computer interface for cursor control. Electroencephalogr. Clin. Neurophysiol. 78 (3), 252–259.

Wolpaw, J.R., McFarland, D.J., 2004. Control of a two-dimensional movement signal by a noninvasive brain-computer interface in humans. Proc. Natl. Acad. Sci. 101 (51), 17849–17854.

Wu, W., Black, M.J., Gao, Y., Bienenstock, E., Serruya, M., Donoghue, J.P., 2002. Inferring hand motion from multi-cell recordings in motor cortex using a

Kalman filter. In: SAB'02-Workshop on Motor Control in Humans and Robots: On the Interplay of Real Brains and Artificial Devices.
Wu, W., Gao, Y., Bienenstock, E., Donoghue, J.P., Black, M.J., 2006. Bayesian population decoding of motor cortical activity using a Kalman filter. Neural Comput. 18 (1), 80–118.
Wu, W., Hatsopoulos, N.G., 2008. Real-time decoding of nonstationary neural activity in motor cortex. IEEE Trans. Neural Syst. Rehabil. Eng. 16 (3), 213–222.
Yoo, S.S., Fairneny, T., Chen, N.K., Choo, S.E., Panych, L.P., Park, H., Lee, S.Y., Jolesz, F.A., 2004. Brain-computer interface using fMRI: spatial navigation by thoughts. Neuroreport 15 (10), 1591–1595.